Magnetic properties of Dashing Rocks loess at Timaru, South Island, New Zealand

Mingming Ma,[1,2] Xiuming Liu,[3,4] Brad J. Pillans,[5] Shouyun Hu,[1] Bin Lü[3] and Huifeng Liu[6]

[1]*State key Laboratory of Lake Science and Environment, Nanjing Institute of Geography and Limnology, Chinese Academy of Sciences, Nanjing 210008, China*
[2]*University of Chinese Academy of Sciences, Beijing 100049, China*
[3]*School of Geographical Sciences, Fujian Normal University, Fuzhou 350007, China. E-mail: xliu@fjnu.edu.cn*
[4]*Department of Environment and Geography, Macquarie University, NSW 2109, Australia*
[5]*Research School of Earth Sciences, Australian National University, Canberra, ACT 0200, Australia*
[6]*Key Laboratory of West China's Environmental Systems, Ministry of Education, Research School of Arid Environment & Climate Change, Lanzhou University, Lanzhou 730000, China*

SUMMARY

The relationships between magnetic susceptibility and pedogenic development are different in various regions of the world. For example, loess magnetic susceptibility shows a positive correlation with pedogenic development in Chinese Loess Plateau (CLP), while it displays a negative correlation with pedogenesis in Alaska and Siberia. To better understand the relationship between magnetic properties and pedogenic development, detailed sampling of Dashing Rocks loess section at Timaru, South Island, New Zealand, was carried out. Multiproxy magnetic parameters such as magnetic susceptibility, anhysteretic remanent magnetization, magnetic hysteresis loops, M_s–T curves and κ–T curves were measured. The results show that the types of magnetic minerals are similar to CLP: magnetite, maghemite, goethite and hematite. However, great differences are found in their concentration: most minerals in the Dashing Rocks section are hard magnetic, such as goethite, the content of paramagnetic minerals is rather high, while the soft-magnetic mineral content is very low. Hard-magnetic and paramagnetic minerals increase with depth, but soft-magnetic minerals decrease with depth, and are absent in the lower part of the profile. Gammate soil structures and Fe/Mn nodules (or pans) are commonly observed in the section, indicating that high susceptibility magnetite and maghemite have been converted to goethite and migrated downward to enrich certain horizons during chemical weathering. This process leads to lower magnetic susceptibility values, possibly related to the source and the transformation of soft-magnetic minerals in a high soil moisture environment. The relationship between magnetic susceptibility and pedogenic development in Dashing Rocks loess section is therefore different from the simple positive and negative relationships in CLP and Siberia, respectively. The more complex relationships between magnetic properties and pedogenic development in New Zealand loess may be related to differing degrees of magnetic mineral transformation at different depths and at different times.

Key words: Environmental magnetism; Rock and mineral magnetism; New Zealand.

1 INTRODUCTION

Since magnetic parameters were introduced into loess study as an effective proxy to reconstruct palaeoenvironmental changes, there have been significant achievements (Liu *et al.* 1985; Kukla *et al.* 1988; Banerjee *et al.* 1993; Heller & Evans 1995; Maher 1998; Maher & Thompson 1999; Evans & Heller 2001; Kemp 2001; Deng

et al. 2005). Magnetic susceptibility (χ) has been particularly successful as a sensitive indicator of the intensity of the ancient summer monsoon on the Chinese Loess Plateau (CLP), because there is a clear positive correlation between χ values and modern precipitation (Zhou *et al.* 1990; Liu *et al.* 1992; Lü *et al.* 1994; Maher *et al.* 1994; Evans & Heller 2001; Chen *et al.* 2005; Hao & Guo 2005). A similar relationship was also observed in the mid-west USA (Geiss

& Zanner 2007; Geiss *et al.* 2008), reflecting the formation of ul-trafine particles of maghemite/magnetite and hematite under warm humid conditions (Zhou *et al.* 1990; Liu *et al.* 1992; Maher *et al.* 1994; Chen *et al.* 2005; Hao & Guo 2005). Based on this widely accepted hypothesis, Orgeira *et al.* (2011) presented a quantitative model for the climatic dependence of magnetic enhancement in loessic soils. Thus, on the CLP, the content of newly formed miner-als has a close linkage with climate and reflects the degree of pedo-genic development in the loess. However, the relationships between χ values and pedogenic development are different in other areas. For instance, in Siberia and Alaska, χ values in loess are higher than in palaeosols (Begét *et al.* 1989; Chlachula *et al.* 1998; Lagroix & Banerjee 2002, 2004; Zhu *et al.* 2003; Kravchinsky *et al.* 2008). Two major hypotheses have been proposed to explain this magnetic depletion mechanism in palaeosols: one is 'wind vigor', and the other is 'gleying'. The 'wind vigor' mechanism can be explained by the strong activity of winds during glacial periods, which can transport and deposit more and heavier magnetic particles (Begét *et al.* 1989; Chlachula *et al.* 1998; Matasova *et al.* 2001; Zhu *et al.* 2003; Kravchinsky *et al.* 2008); and is supported by wind tunnel ex-periments (Begét *et al.* 1990). In contrast, other investigators believe that chemical weathering, in particular pedogenic 'gleying', plays an important role in Siberia and Alaska, which results in a decrease of magnetic minerals (Maher 1998; Evans & Heller 2001; Liu *et al.* 2007, 2008). The phenomenon that strong pedogenic development can weaken χ was also detected in other areas (Bidegain *et al.* 2005, 2009, Bidegain & Rico 2012; Ma *et al.* 2012). Furthermore, in other studies, the relationships between loess χ and climate state are more complicated: either unclear or were not observed (Pillans & Wright 1990; Sun & Liu 2000; Carter-Stiglitz *et al.* 2006; Heil *et al.* 2010). Therefore, loess magnetic properties are different in different regions, indicating that the application of χ has its limi-tations, and this makes the effectiveness of χ as a palaeoclimatic indicator complex. So only when we fully understand the mecha-nisms that control χ, can we better understand its real significance in relation to palaeoenvironmental changes.

New Zealand is a group of islands located at mid-latitudes in the Southern Hemisphere, the two main islands being the South Island and North Island. The climate is temperate maritime, and the annual precipitation is generally high. Loess is widely distributed in New Zealand, with loess deposits thicker than 1 m accounting for about 15 per cent of the island area (Bruce *et al.* 1973; McCraw 1975). In recent years, the study of loess magnetic properties has been mainly concentrated in the Northern Hemisphere, but very few in the Southern Hemisphere. The extensive distributed loess in New Zealand therefore provides a valuable archive for loess study in the Southern Hemisphere. This study is based on the magnetic proper-ties of loess from New Zealand, in order to explore the similarities and differences of magnetic susceptibility change mechanisms be-tween the two hemispheres, and try to get a more comprehensive understanding of global mechanisms.

2 MATERIALS AND METHODS

The study profile is near the city of Timaru, in the South Island of New Zealand, at a site called Dashing Rocks (Fig. 1). The modern annual rainfall is 550 mm, and the annual temperature is about $11°$C (Runge *et al.* 1974). The total thickness of the profile is 8 m or so, including the present soil layer, three palaeosol layers and four loess layers. For details, see Tonkin *et al.* (1974). The uppermost five samples were taken at 10 cm intervals, while others were sampled at

20 cm intervals, and 42 samples were collected in all. In addition, 24 topsoil samples from other South Island locations (with a thickness of at least 40 cm of loess—see Fig. 1 for locations) and samples from Xifeng S5 (CLP) were also collected for comparison. The samples were dried naturally indoors, then gently ground to disaggregate the grains. The samples were then packed into small nonmagnetic plastic boxes ($10\,cm^3$) before measurement.

Magnetic susceptibility (χ_{lf}, χ_{hf}) was measured with a Bartington MS2 meter ($0.47\sim4.7$ kHz) and then determined by mass normal-ization method. Frequency-dependent susceptibility (χ_{fd} per cent) was calculated: χ_{fd}(per cent) $= ((\chi_{lf} - \chi_{hf})/\chi_{lf}) \times 100$. Anhys-teretic remanent magnetization (ARM) was measured using a Min-ispin Magnetometer after demagnetization with a DTECH alter-nating field (AF) demagnetizer. The peak AF used was 100 mT and the DC bias field was 0.1 mT. Isothermal remanent magnetiza-tion (IRM) and saturated isothermal remanent magnetization SIRM (IRM 1T) were acquired by using a MMPM10 pulse magnetizer and Molspin Minispin magnetometer. The backfield remagnetiza-tion of SIRM was carried out using reverse fields at 10 mT steps and remanence coercivity (H_{cr}) was calculated using linear inter-polation. Thermomagnetic curves and magnetic hysteresis loops were measured with a variable field translation balance (VFTB); the thermomagnetic curves were completed in air, then hystere-sis loops were corrected for paramagnetic contributions. Hysteresis parameters, including saturation magnetization (M_s), remanent sat-uration magnetization (M_{rs}) and coercivity (B_c) were determined from corrected loops. Magnetic susceptibility versus temperature curves ($\kappa–T$) were obtained from room temperature to $700°$C and back to room temperature using a KLY 3 Kappa bridge with a CS-3 high-temperature furnace in an argon atmosphere. Grain size was measured using a Mastersizer 2000 laser particle size analyzer. The content of calcium carbonate ($CaCO_3$) was determined by the gasmetric method: weighed suitable samples and standard pure cal-cium carbonate samples were reacted with HCl and the volumes of generated CO_2 were measured. The content of $CaCO_3$ was then calculated as follows:

$$CaCO_3\% = m_{standard} \times V_{sample} \times 100 / (V_{standard} \times m_{sample}),$$

where $m_{standard}$ and m_{sample} are the mass of standard pure calcium carbonate and loess samples, respectively, $V_{standard}$ and V_{sample} are the volumes of CO_2 generated by standard pure calcium carbonate and loess samples, respectively.

The raw data were analyzed using Microsoft Office Excel 2007. All the measurements above were completed in the Key Laboratory of West China's Environmental Systems, Ministry of Education, Lanzhou University.

3 STRATIGRAPHIC CHARACTERISTICS

According to the stratigraphic classification used by Tonkin *et al.* (1974), Dashing Rocks profile can be divided into four layers, called Loess Member 1, Loess Member 2, Loess Member 3 and Loess Member 4, respectively (see Fig. 2), and these four layers are col-lectively called 'Dashing Rocks Formation'. Each loess member has two broad components: an upper unit with clay loam to silty clay loam texture, blocky structure, colour mottling and fine Fe/Mn concretions, and a lower unit characterized by silty loam texture and a very dense, coarse prismatic structure (fragipan) with a prominent polygonal pattern of vertical veins. While acknowledging that both upper and lower parts have been affected by pedogenic processes,
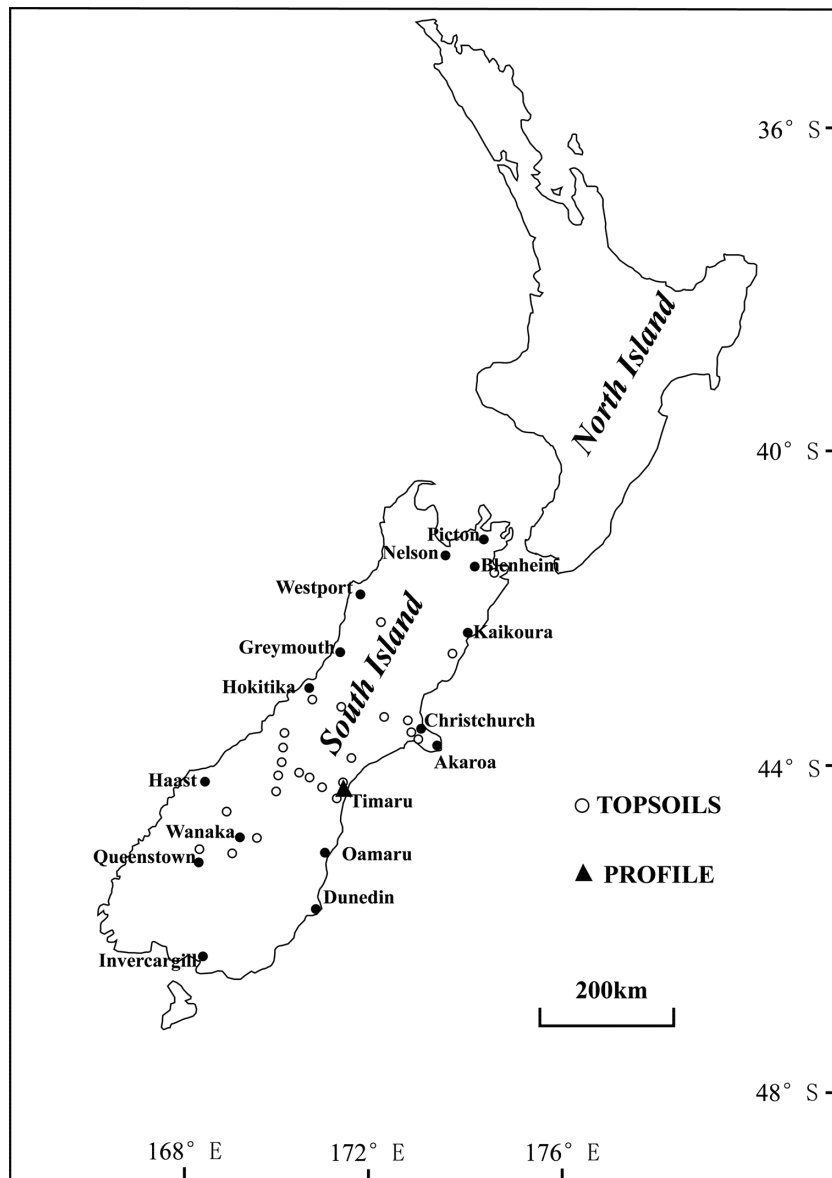
Figure 1. Locations of study profile and topsoils.

for simplicity we refer to the upper parts as palaeosol or soil layers and the lower parts as loess layers.

Just south of Timaru, where the loess thickness is greater, Tonkin *et al.* (1974) and Runge *et al.* (1974) described a series of large diameter borehole cores (Darling Holes) through the loess and showed the occurrence of two older loess layers, which they named Loess Member 5 and Loess Member 6. Berger *et al.* (2001) carried out a systematic chronological study of loess in the Timaru region, which is summarized here:

(1) A widespread volcanic ash layer (Kawakawa Tephra) at a depth of 1.1 m in Loess Member 1 has a radiocarbon age of c. 25 ka (Vandergoes *et al.* 2013).

(2) The basal part of Loess Member 1 yielded a thermoluminescence (TL) age of 63.5 ± 6.9 ka.

(3) Peat at the base of Loess Member 1 has a radiocarbon age of >50 ka and a pollen content consistent with a last interglacial age, c, 120 ka.

(4) TL ages of 155 ± 19 ka and 162 ± 31 ka were obtained from the upper and lower parts, respectively, of Loess Member 2.

All the loess sections studied by Tonkin *et al.* (1974), Runge *et al.* (1974) and Berger *et al.* (2001) are in close proximity and individual loess members can be confidently correlated between sections. Accordingly, in Fig. 2, we summarize the stratigraphy and chronology of Timaru loess sections, and show a tentative correlation between loess stratigraphy and marine isotope stages (MIS), noting the striking similarity between total phosphorus content of the loess (Runge *et al.* 1974) and the MIS record, with palaeosols characterized by decreasing *P* content with depth and the basal parts of loess members having high *P* as a result of preferential loss and leaching of *P* during pedogenesis. We, therefore, estimate that the bottom of Dashing Rocks profile is not older than 400 ka. The age of the basalt under loess deposits is K/Ar dated at 2.47 Ma (Mathews & Curtis 1966), equivalent to 2.54 Ma based on revised decay constants (Dalrymple 1979).
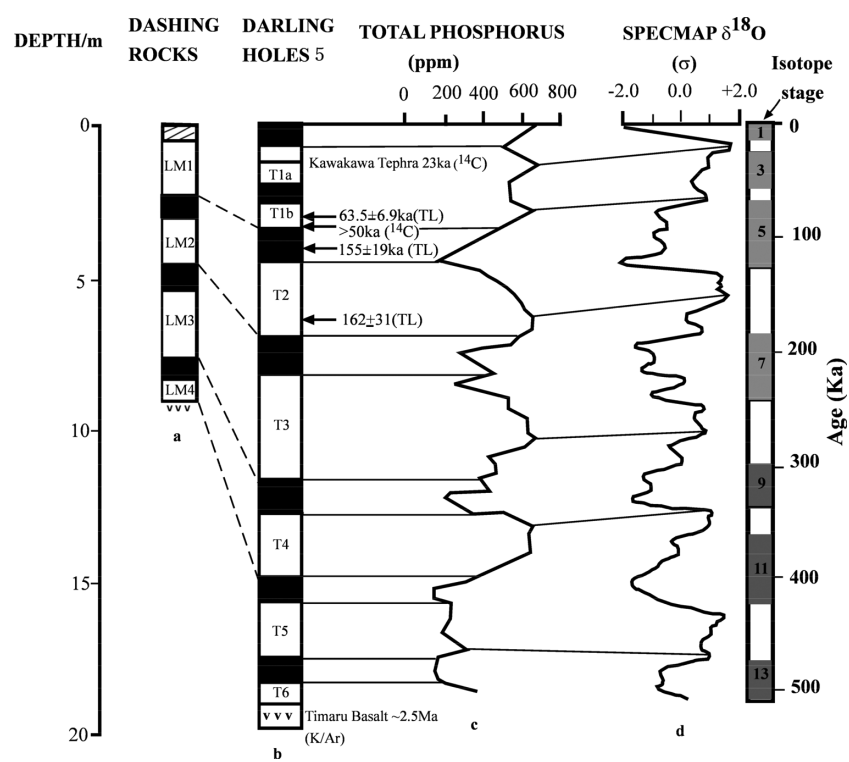
Figure 2. Stratigraphy of Dashing Rocks section (a) and Darling Holes 5 section (b), content of total phosphorus of Darling Holes 5 (c), and the Marine Oxygen Isotope (MIS) record (a and b are from Tonkin *et al.* (1974), c is from Runge *et al.* (1974), d is from Imbrie *et al.* (1984).

4   RESULTS

4.1   Conventional magnetic and nonmagnetic parameters

The overall χ_{lf} values in Dashing Rocks profile are low (Fig. 3a), varying between a maximum value of 12.13×10^{-8} m^3 kg^{-1} and a minimum of 5.82×10^{-8} m^3 kg^{-1}, which is far lower than that of Xifeng profile (Fig. 3g), and indicating that the content of magnetic minerals in Dashing Rocks samples is very low. Furthermore, the variations of χ_{lf} have an unclear relationship with the degree

of pedogenic development (strength): except for the first palaeosol layer and the second loess layer, which have magnetic susceptibility peaks, the χ_{lf} values of other layers are similar. χ_{fd} per cent fluctuates irregularly from 5 to 12 per cent, and has no relationship with χ_{lf} or pedogenic strength, probably because at such low χ_{lf} values, χ_{fd} per cent has lost its climatic significance (Dearing *et al.* 1996; Hu 1998).

ARM is mainly carried by single domain (SD) and pseudo single domain (PSD) magnetic particles, so ARM can reflect the content of
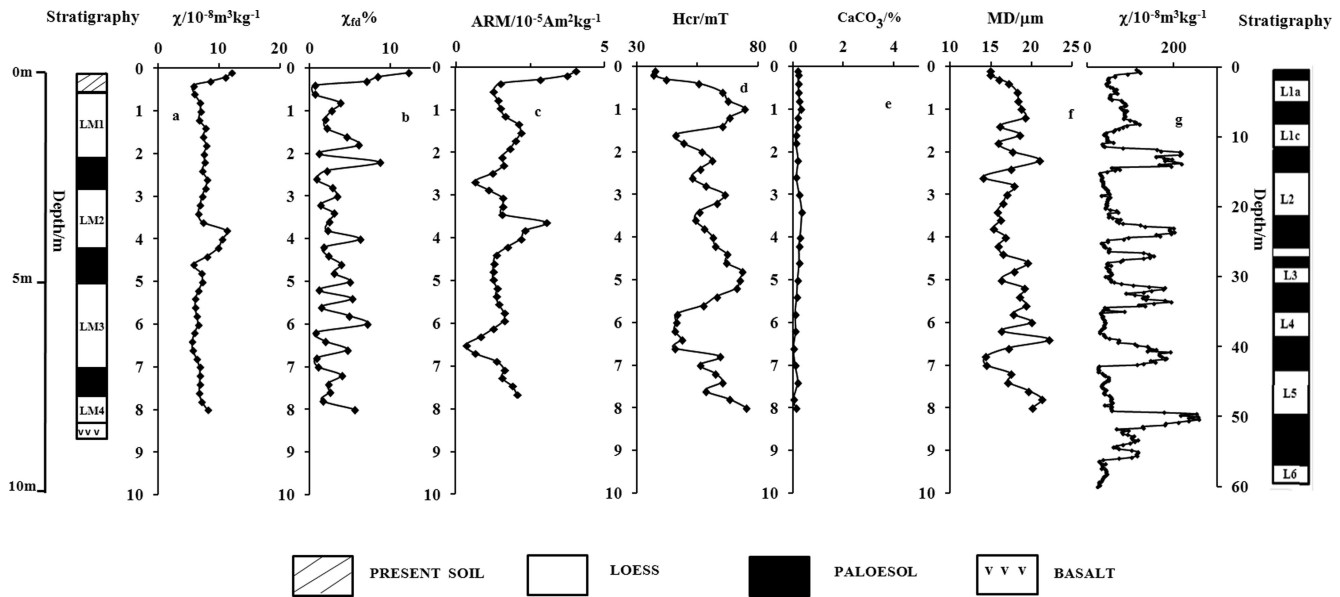

Figure 3. Comparison of magnetic parameters from Dashing Rocks and Xifeng. (a) χ_{lf} of Dashing Rocks, (b) χ_{fd}% of Dashing Rocks, (c) ARM of Dashing Rocks, (d) H_{cr} of Dashing Rocks, (e) CaCo$_3$ per cent of Dashing Rocks, (f) median diameter (Md) of Dashing Rocks and (g) χ_{lf} of Xifeng.

Table 1. Location and χ_{lf} values of topsoil samples, South Island, New Zealand.

Position	$\chi_{lf}/10^{-8}$ m^3 kg^{-1}	Position	$\chi_{lf}/10^{-8}$ m^3 kg^{-1}	Position	$\chi_{lf}/10^{-8}$ m^3 kg^{-1}
41°39′S, 174°3′E	59.50	44°34′S, 169°45′E	21.50	44°5′S, 170°49′E	8.21
42°44′S, 173°16′E	10.22	44°29′S, 169°1′E	15.36	44°18′S, 171°55′E	15.86
43°14′S, 171°42′E	14.85	44°11′S, 170°7′E	14.98	44°34′S, 171°6′E	6.19
42°49′S, 170°57′E	0.22	44°6′S, 170°7′E	17.15	44°24′S, 171°14′E	16.43
44°27′S, 169°20′E	24.50	44°1′S, 170°7′E	13.96	43°3′S, 171°37′E	10.18
44°56′S, 168°39′E	29.57	43°57′S, 170°7′E	8.33	43°39′S, 172°32′E	13.16
44°50′S, 169°13′E	54.42	43°52′S, 170°7′E	7.57	43°41′S, 172°33′E	66.11
44°46′S, 169°38′E	11.63	44°0′S, 170°29′E	19.32	43°46′S, 172°39′E	12.51
All	24	Mean value of χ_{lf}		19.65×10^{-8} m^3 kg^{-1}	

SD and PSD magnetic particles. In Dashing Rocks profile, there is a positive relation between ARM and χ_{lf}, suggesting that SD and PSD magnetic particles make an important contribution to χ_{lf}. The values of H_{cr} mainly reflect the relative content of hard-magnetic minerals. In Dashing Rocks profile, H_{cr} varies from 30 to 75 mT (Fig. 3d), and most samples have a value higher than 50 mT. Furthermore, H_{cr} increases with depth, implying that the content of hard-magnetic minerals also increases with depth. However, there are no clear relationships among H_{cr}, χ_{lf} and pedogenic strength. The content of CaCO$_3$ is low in all samples (Fig. 3e), indicating that leaching was sufficiently strong that CaCO$_3$ has been almost removed from the whole section. Median grainsize diameter (Md) changes little in the whole profile (Fig. 3f), and the values fluctuate between 10 to 20 μm. Furthermore, there is also no relation between Md and χ_{lf} or pedogenic strength, implying that Md and χ_{lf} cannot be used as effective climatic indicators as in CLP. χ_{lf} values of topsoils from other South Island locations are shown in Table 1.

4.2 Magnetic hysteresis loops and thermomagnetic curves

Magnetic hysteresis loops contain a wealth of information, such as saturated magnetization (M_s), saturated isothermal remnant magnetization (M_{rs}), coercivity (H_c) and remnant coercivity (H_{cr}), and can be used to identify whether the magnetic mineralogy is soft or hard, and even the size of magnetic particles. Thermomagnetic (M_s–t) curves can be used to determine the Curie temperature (T_c), and because different minerals have different T_c, so we can distinguish the types of magnetic minerals. The $M_s(t)$ curves were completed in air. The measured samples, from Dashing Rocks section, are 38NZ7 (loess sample, depth = 0.8 m), 38NZ15 (palaeosol sample, depth = 2.4 m), 38NZ22 (loess sample, depth = 3.8 m), 38NZ27 (palaeosol sample, depth = 4.8m), 38NZ34 (loess sample, depth = 6.2 m), 38NZ37 (loess sample, depth = 6.8 m).

All magnetic hysteresis loops show that most magnetic minerals are paramagnetic or hard magnetic (Fig. 4). Although the loops were closed under 300 mT, indicating the existence of soft-magnetic minerals, the linear increasing trend above 300 mT (occupying the main part of the loops), suggests that there are more paramagnetic or hard-magnetic minerals. Samples 7, 15, 22 and 27 are from the upper part of the profile: their magnetic hysteresis loops show the same shape, and there are indications of soft-magnetic minerals, but in the lower part, such as sample 34, the signal of soft-magnetic minerals is very weak, while in the deepest sample (38NZ37), the signal has almost disappeared. Although hard-magnetic minerals are dominant, magnetic hysteresis loops (Fig. 4, 7→15→22→27→34→37) show that the content of soft-magnetic minerals slightly reduces while the content of hard-magnetic minerals increases with depth. As a result, at the bottom of the profile, the content of soft-magnetic minerals is extremely low.

The corrected hysteresis loops in Fig. 5 show that the loops of the upper four samples (7, 15, 22 and 27) are characteristic of soft-magnetic minerals, their H_c values are low and they have higher M_s values. While the loops of the lower two samples (34, 37) show obvious differences: their curves are characteristically wasp-waisted, indicating that the ratio of soft- to hard-magnetic minerals reaches a certain range (Roberts *et al.* 1995; Tauxe *et al.* 1996), especially in sample no. 37. In addition, these two samples have higher H_c values and lower M_s values, a change that has a broad similarity with χ_{lf}, with χ_{lf} values in the upper part being generally higher than in the lower part. The boundary between the upper and lower parts is about 5 m. These clear changes in hysteresis loops also suggest that the ratio of soft- to hard-magnetic minerals varies with depth, i.e. in the lower part of the profile, soft-magnetic minerals are reduced while hard-magnetic minerals increase.

In Fig. 6, the $M_s(t)$ curves, and the corresponding magnetic hysteresis loops in Figs 4 and 5, belong to the same samples. In order to prevent the signal of paramagnetic minerals from masking the soft- and hard-magnetic minerals, all $M_s(t)$ curves have been corrected by subtracting the paramagnetic signal. Heating curves of all samples show turning points at 120 and 670°C. The turning point at 120°C is generally explained by the dehydration of goethite (Vander 1951), while 670°C is close to the Neel temperature of hematite. However, most of the hematite is likely to be the end product of goethite thermal decomposition, because before heating the sample colour was yellow to slightly green, while after heating the colour is red, consistent with formation of hematite in the heating process. $M_s(t)$ curves of the upper samples (7, 15, 22 and 27) also have a turning point at 580°C, implying the presence of magnetite. However, in the lower two samples (34 and 37), there is no magnetite signal, but the singals of goethite and hematite have been enhanced. So, the closed hysteresis loops under 300 mT are mainly caused by magnetite. These changes of $M_s(t)$ curves are consistent with the magnetic hysteresis loop: as depth increases, soft-magnetic minerals are reduced and dissolved while paramagnetic or hard-magnetic minerals increase.

Most samples that have been reported from CLP contain maghemite, which is usually thermally unstable (Liu *et al.* 1985; Liu *et al.* 1999) and $M_s(t)$ curves from CLP are always irreversible, marked by the partial loss of magnetization. Liu *et al.* (1999) used the difference of magnetization (ΔM_s) before and after heating to describe the content of maghemite: ΔM_s increases with the enhancement of pedogenesis (increase of χ_{lf}) in Luochuan profile, indicating that there is a close relationship between the increases of maghemite and the pedogenesis process. However, in Dashing Rocks profile, some samples display heating curves that are below their cooling curves (Fig. 6; no. 7, 34 and 37), possibly because some weak magnetic or paramagnetic minerals were transformed to strong magnetic minerals resulting in the enhancement of
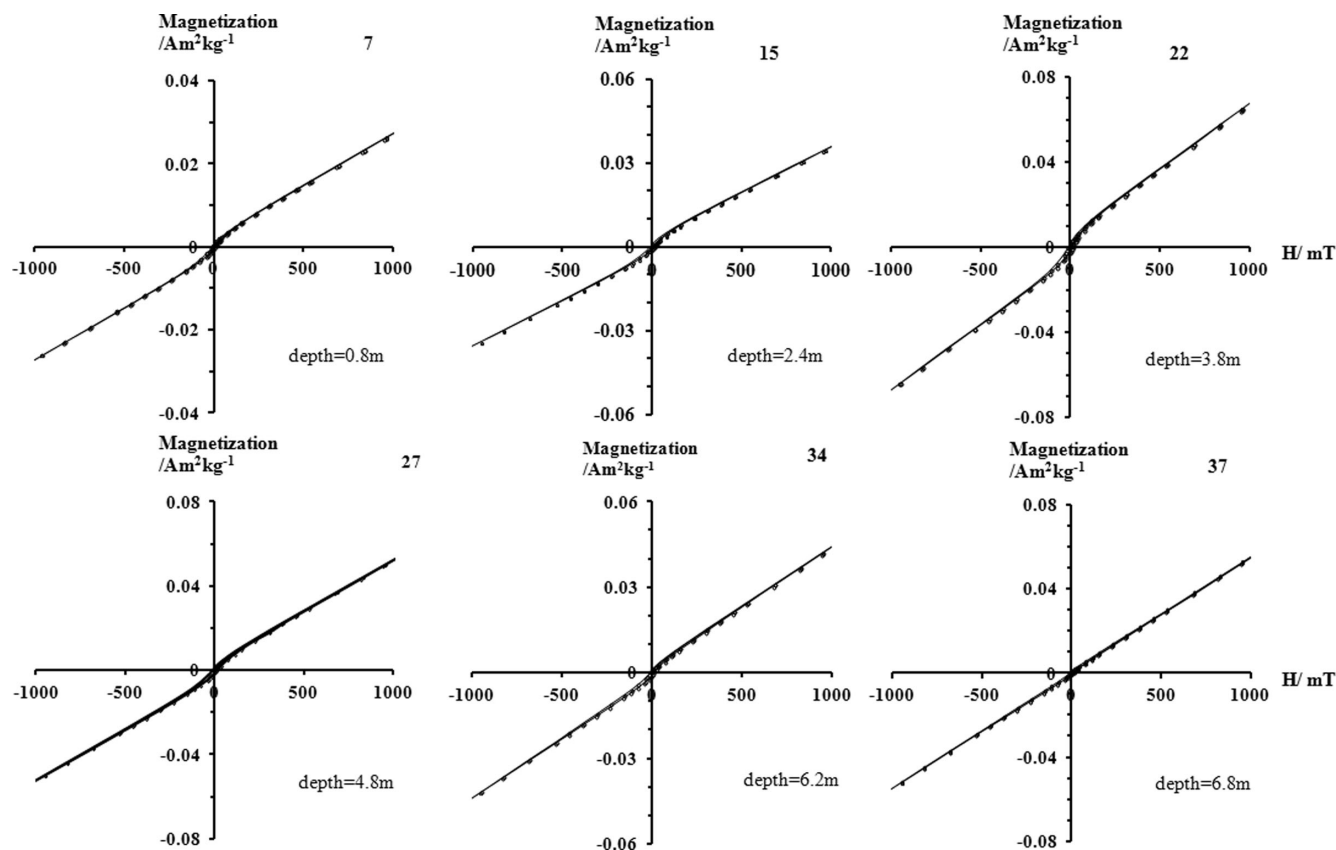
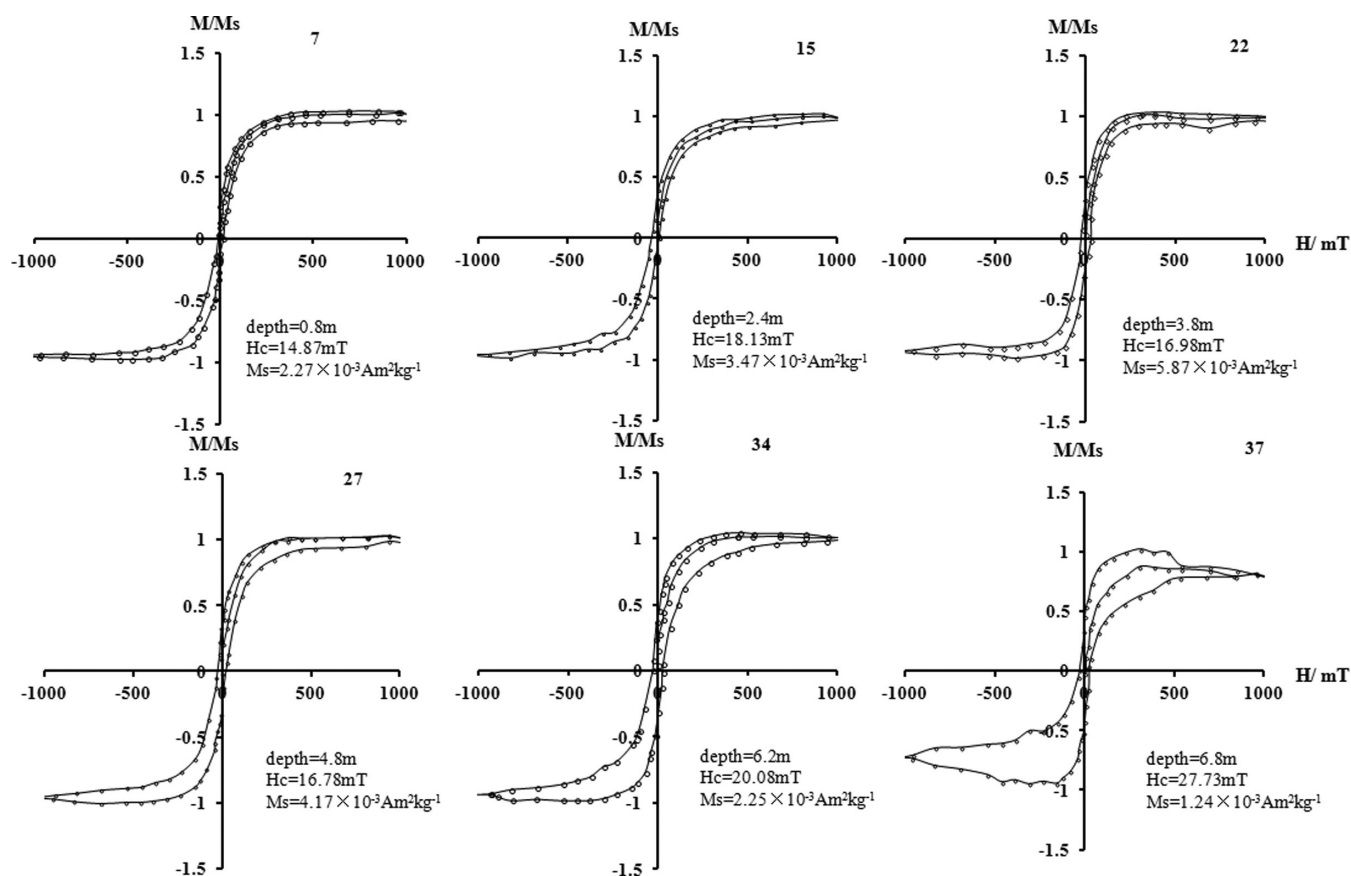**Figure 4.** Magnetic hysteresis loops of typical samples in Dashing Rocks profile.

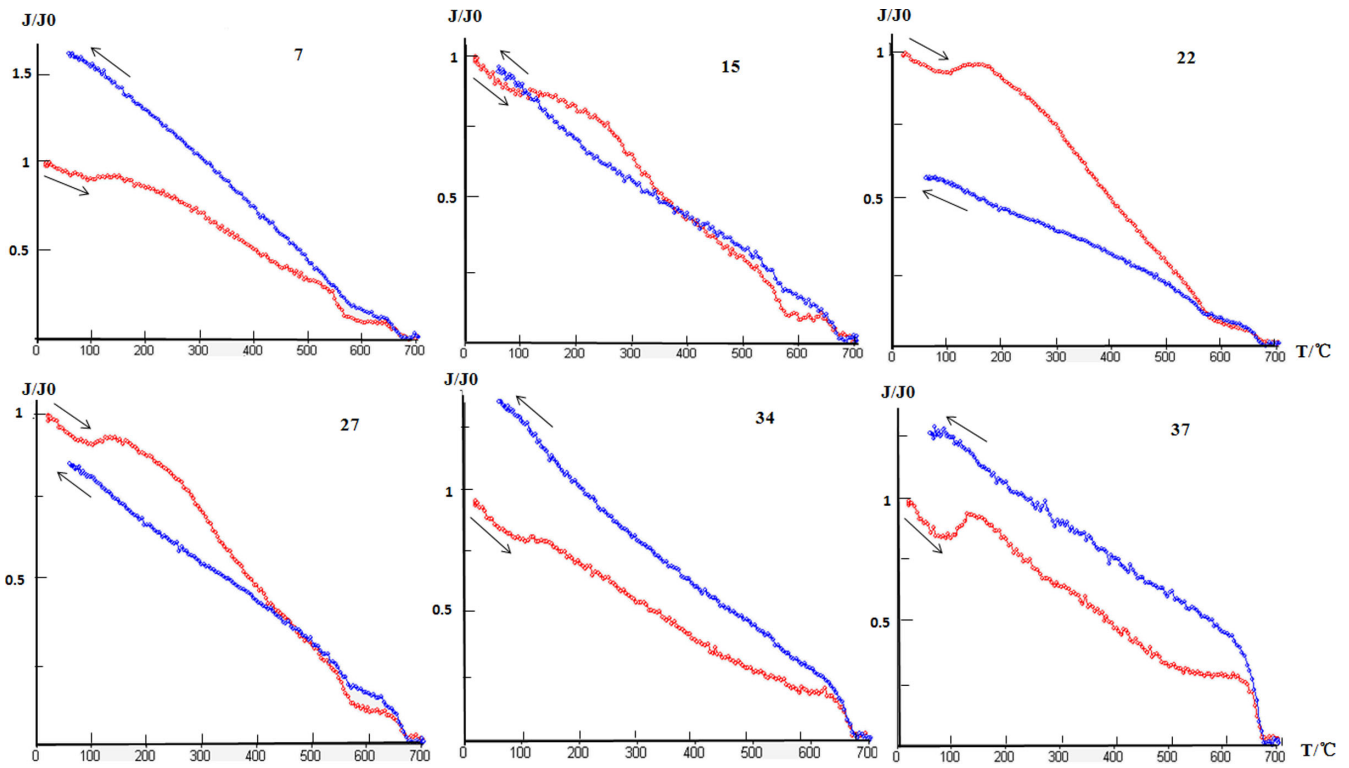**Figure 5.** Corrected hysteresis loops of the same samples in Fig. 4.

Figure 6. $M_s(t)$ curves of typical samples in Dashing Rocks profile (the applied field is about 110 mT).

magnetization after heating (Zhu *et al.* 2001), while samples no. 22, 27 display cooling curves below their heating curves, and sample no. 15 shows that ΔM_s before and after heating is almost zero. So in Dashing Rocks profile there is no relationship between ΔM_s and χ_{lf}. Furthermore, there is no typical Tc of maghemite in most samples (Fig. 6), indicating that there is little or no maghemite. We, therefore, conclude that there are significant differences in the magnetic mineral composition between Dashing Rocks and CLP.

As Fig. 6 shows, goethite decay can be clearly seen in the M_s–T curves after paramagnetic correction. Thus, soft-magnetic minerals (such as magnetite) have an insignificant influence on magnetization between room temperature and 120°C, and they can be ignored. So in order to semiquantify the goethite content, we express the goethite component as a percentage of the total magnetic component as:

$$\Delta M_s\,(\%) = (\Delta M_{s-room} - \Delta M_{s-120})/\Delta M_{s-room} \times 100\,,$$

where ΔM_{s-room} and ΔM_{s-120} represent the magnetization at room temperature and 120°C in M_s–T heating curves, respectively, and we obtain a good inverse correlation between ΔM_s (per cent) and susceptibility (Fig. 7). This implies that as susceptibility decreases, the goethite contributes an incremental fraction of the magnetic component. This is consistent with the magnetic hysteresis loops and M_s–T curves: the decrease of χ_{lf} is due to the decrease of soft-magnetic minerals (magnetite) and the increase of hard-magnetic minerals (goethite).

4.3 Magnetic susceptibility versus temperature (κ–T) curves

Compared with M_s–T curves, κ–T curves are affected by magnetic mineral type and particle size at the same time, so κ–T curves are more sensitive to slight changes of magnetic minerals during the heating process (Liu *et al.* 2005). All κ–T curves, shown in Fig. 8,
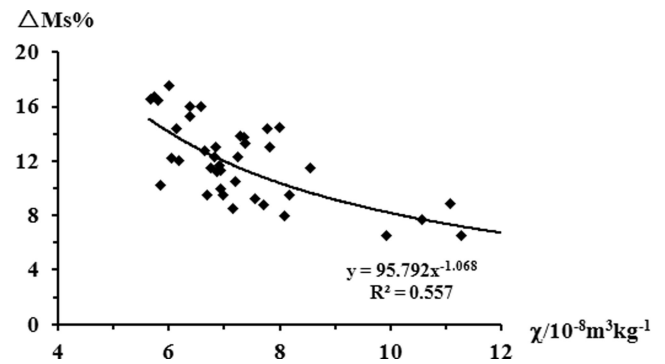

Figure 7. Correlation between magnetic susceptibility and ΔM_s (per cent).

are for the same samples as the M_s–T curves. Obviously, the curves of samples 7, 15 and 27 have a similar shape: the heating curve has a peak between 500 and –600°C, indicating the production of strong magnetic minerals, and the T_c of 580°C in heating and cooling curves suggests the presence of magnetite. In addition, there is a turning point near 500°C in the cooling curve, a phenomenon that was also reported by Minyuk *et al.* (2011), but they did not give any explanation. Whether this turning point is the Curie point of a new mineral, or in part reflects a Hopkinson peak needs further confirmation. χ_{lf} values steadily decline in the cooling curve from 400°C to room temperature. This is caused by the slowing down of particle vibration as the temperature decreases, and makes the relaxation time increase so that SP particles change to SD particles, leading to lower χ_{lf}. The κ–T curves of samples 22, 34 and 37 are similar: strong magnetic minerals were also generated during heating, but there is no turning point near 500°C except for the T_c of 580°C. What is more, χ_{lf} values steadily increase from 580°C to room temperature.
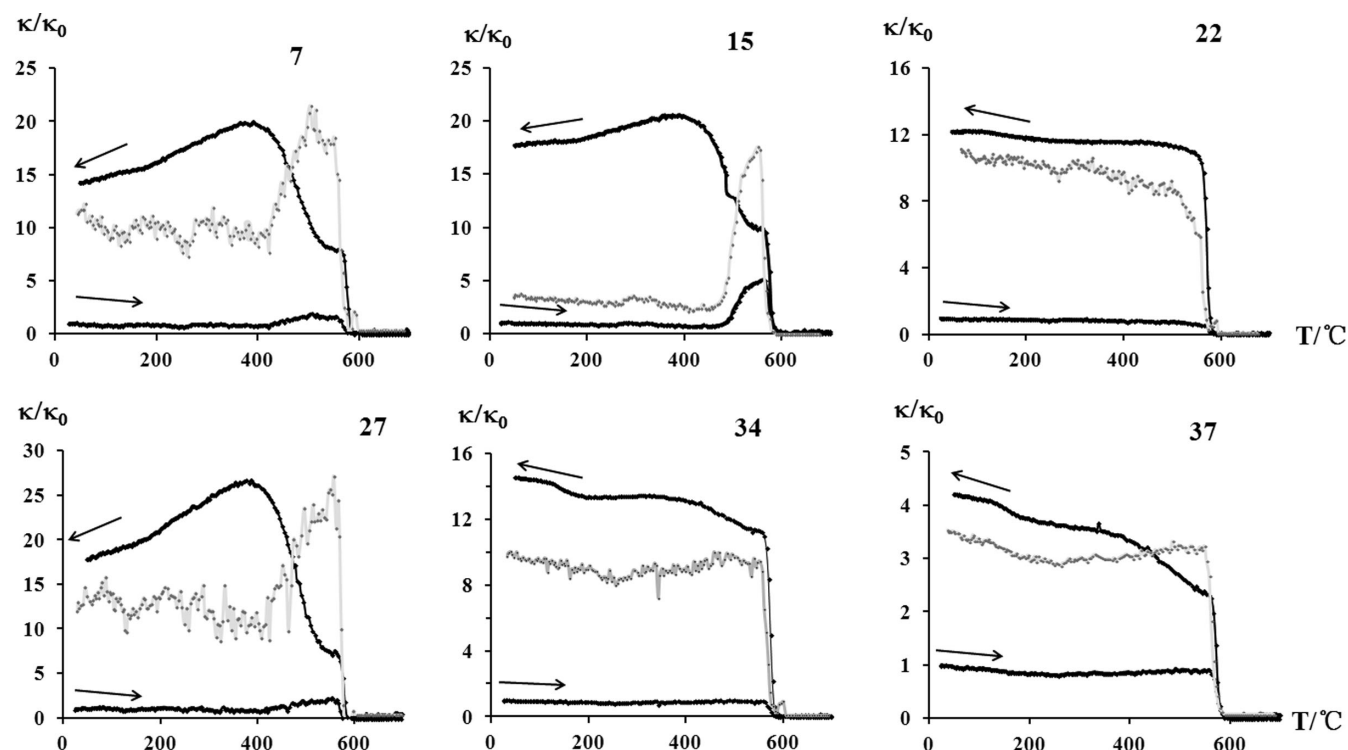
Figure 8. κ–T curves of typical samples in Dashing Rocks profile (grey lines represent the heating curves, but their *y*-axes are not shown).

5 DISCUSSION

The above magnetic parameters suggest that the types of magnetic minerals in the Dashing Rocks loess profile are similar to those in CLP, but they are present in different proportions: in CLP, magnetic minerals are mainly soft-magnetic (such as magnetite and maghemite) and the content of hard-magnetic minerals (such as hematite, goethite) is very low. In contrast, in Dashing Rocks profile, the dominant minerals are hard and paramagnetic, whereas soft-magnetic minerals are minor, and only occur in the upper part. The content of magnetic minerals in Dashing Rocks is also far lower than that in CLP.

5.1 Reasons for low χ_{lf}

Generally speaking, the χ of all loess-palaeosol sequences can be divided into two parts: primary and secondary. The primary part relates to source minerals, while the secondary part relates to the degree of pedogenic modification after deposition. The overall χ_{lf} value in Dashing Rocks profile is low (Fig. 3a)—the maximum value is 12.13×10^{-8} m^3 kg^{-1} and the minimum is 5.82×10^{-8} m^3 kg^{-1}, which is far lower than that of Xifeng profile (Fig. 3g), with a maximum value for palaeosols of 256×10^{-8} m^3 kg^{-1} and a minimum for loess of 30×10^{-8} m^3 kg^{-1}. In CLP, χ_{lf} has a close relation with annual rainfall, so χ_{lf} enhancement is interpreted to represent the formation of ultrafine particles of maghemite/magnetite and hematite under suitable moisture and temperature conditions (Zhou *et al.* 1990; Liu *et al.* 1992; Maher *et al.* 1994; Chen *et al.* 2005; Hao & Guo 2005). However, the relationship between χ_{lf} and annual rainfall is not always positive—if rainfall is too high, effective soil moisture becomes excessive, which can lead to the dissolution and transformation of magnetic minerals, and therefore χ_{lf} will decrease with increasing of rainfall (Liu *et al.* 2007; Ma *et al.* 2012). For example, the annual rainfall of Mackenzie's Waterholes

Creek (MWC) loess profile in Australia is 924.2 mm, and under these conditions magnetic minerals have been dissolved and transformed (Ma *et al.* 2012). Despite the fact that mean annual rainfall at Dashing Rocks being only 550 mm, with a mean annual temperature of 11°C, Fe/Mn nodules are common throughout the section, indicating that it experienced significant chemical weathering of Fe-bearing minerals.

The content of CaCO$_3$ in all samples is near zero (Fig. 3e), which also indicates strong profile leaching. Xia *et al.* (1993) measured various oxide ratios of loess deposits in the South Island, and their results also showed that the leaching and movement of elements is stronger than that in CLP. Therefore, profile leaching may explain dissolution of Fe oxides (such as magnetite and maghemite) to goethite and explain the low χ_{lf} at Dashing Rocks, despite the low mean annual rainfall of 550 mm. This can be confirmed by Fig. 7, which shows that χ_{lf} has a negative relation with the contribution of goethite, suggesting that the more magnetite transformed to goethite, the lower is the χ_{lf}.

Concerning source minerals, if the χ_{lf} of loess source material is very low, then it will favour low χ_{lf} in resultant loess deposits. The χ_{lf} values of top soils we sampled in South Island have a mean χ_{lf} of 19.65×10^{-8} m^3 kg^{-1}, and only five samples are more than 20×10^{-8} m^3 kg^{-1} (Table 1) and they are far lower than those of top soils in CLP (Xia *et al.* 2012). The source of Chinese loess is controversial—An *et al.* (2000) considered that the northern deserts, especially the Gobi, have been the major loess source, and Sun *et al.* (2008) concluded that the far-travelled dust derived mainly from the Gobi Desert and the Badain Juran and Tengger Deserts. On the other hand, Maher *et al.* (2009) suggest that the source areas for the loess encompass a much larger area than any one proximal desert region. Nevertheless, the environment of the Chinese loess source is arid and oxidative, so the magnetic minerals are mainly composed of Fe oxides such as magnetite, maghemite and hematite, and weathering processes are dominated

by physical weathering. In contrast, the Dashing Rocks loess is proximal aeolian-dust from fluvio-glacial outwash plains, alluvial plains or beaches (Xia *et al.* 1993), and the environment is more humid, so Fe oxides are more likely to be dissolved or transformed to Fe hydroxide (such as goethite, limonite). Although the top soil will undergo pedogenic transformations after deposition (in details, see Section 5.2), the evident differences between Chinese topsoil and New Zealand topsoil suggest that different sources maybe an important reason for low χ_{lf} in the Dashing Rocks profile.

Florindo *et al.* (2003) conducted a survey of magnetic susceptibility and pore water geochemical data from Ocean Drilling Program sites, and found that there was a linkage between high dissolved silica concentrations and low magnetic susceptibilities. They suggest that this observed linkage also holds for environments with low biogenic silica productivity but with high interstitial silica concentrations due to dissolution of silicic volcanic ashes. Though volcanic ashes are distributed widely in New Zealand (e.g. including one ash layer in the Darling Holes 5 section in Fig. 2), there was no trace in our samples. We, therefore, conclude that the influence of high dissolved silica concentrations on low χ_{lf}, caused by volcanic ashes, may not be significant in our study.

5.2 Climatic significance

In a comparative study between χ_{lf} and degree of soil development since S5 from Luochuan, Xifeng and Baoji, as well as the study of different kinds of magnetic minerals in loess/palaeosol sequences in Alaska and Siberia, Liu *et al.* (1999, 2007) concluded that there was a pedogenic climatic threshold relating to excessive soil moisture (waterlogging) that makes Fe oxides such as magnetite and maghemite unstable and transform to goethite/limonite (which are stable in excessively humid environments), leading to reduction in χ_{lf}. In Luochuan and Xifeng sections, χ_{lf} reaches highest values in S5 and S1, corresponding to the strongest and the second strongest pedogenic soil layers, respectively. In Baoji, while there is more annual rainfall than in Luochuan and Xifeng, and while S5 is also the strongest pedogenic soil layer, its χ_{lf} is not only the lowest of the younger five palaeosol layers but also it is lower than at the other two sites (Liu *et al.* 2001). According to these studies, Liu *et al.* (1999, 2007) proposed an ideal model to explain this phenomenon: χ_{lf} of loess and palaeosols all over the world can be divided into two parts: primary and secondary. But in different regions, in different profiles or at different times, the relative importance of these two parts is different. In the primary part, magnetite and maghemite make a significant contribution to χ_{lf}, but their content will increase or decrease during pedogenesis depending on local climatic conditions. If pedogenesis occurs in a suitable dry and oxidizing environment, then it will benefit the formation and conservation of magnetite and maghemite leading to an increase in χ_{lf}. This situation is typical of most parts of China, Tajikistan, Serbia and Romania. However, if pedogenesis occurs in an excessively moist environment, primary magnetite and maghemite may be transformed to Fe hydroxides, such as goethite/limonite, and χ_{lf} values will decrease. This model has been confirmed as a mechanism for reducing χ_{lf} values in Siberia (Liu *et al.* 2007) and Australia (Ma *et al.* 2012).

In Dashing Rocks profile, the content of soft-magnetic minerals, showed by magnetic hysteresis loops, is very low, and it decreases with increasing depth (Figs 4 and 5). M_s–T curves also show that the contents of magnetite and maghemite are low, and even absent in the lower part of the profile; the main magnetic mineral is goethite. This phenomenon is very similar to that in the MWC profile, in Australia (Ma *et al.* 2012): from top to bottom, the ratio of soft/hard-magnetic

minerals gradually decreases (as the magnetic hysteresis loops from different depths show in Figs 4 and 5), related to the increase in soil moisture causing the residual Fe oxides (such as magnetite) to be transformed to Fe hydroxides (such as goethite, see Figs 6 and 7).

If we consider the Dashing Rocks profile and MWC profile together, the highest χ_{lf} value is 47×10^{-8} m^3 kg^{-1} and the minimum is 16×10^{-8} m^3 kg^{-1} in MWC (Ma *et al.* 2012), which is higher than that in Dashing Rocks. The magnetic parameters in MWC can be also divided into two parts: χ_{lf} and χ fd per cent are higher in upper part than in the lower part, and H_{cr} is relatively low in the upper part. Ma *et al.* (2012) suggested that the lower part experienced a stronger pedogenesis. Fig. 9 shows the M_s–T curve and magnetic hysteresis loop of a sample from the lower part of MWC profile and there is still a soft-magnetic signal in hysteresis loop. After paramagnetic correction, the presence of magnetite is also indicated by the M_s–T curve. However, in Dashing Rocks, the maximum χ_{lf} is lower than the minimum χ_{lf} in MWC, and soft-magnetic minerals only occur in the upper part (Figs 4–6), indicating that the transformation of soft-magnetic minerals in Dashing Rocks is greater than in MWC. There may be two reasons for the difference: (1) the content of soft-magnetic minerals in the source minerals may be low, even if the strength of transformation after deposition is not very strong; and (2) related to local environmental factors, such as higher soil moisture in the Dashing Rocks profile, resulting in an increase in Fe hydroxides.

From Fig. 3, we know that the variation of χ_{lf} has no clear relationship with pedogenic strength in Dashing Rocks profile: except for the first palaeosol layer and the second loess layer that have χ_{lf} peaks, the χ_{lf} values of other layers are similar. Besides, there is also no relation between median grainsize and χ_{lf} /pedogenic strength, implying that in the relatively cooler and drier period of loess deposition, stronger winds did not transport coarser particles, so χ_{lf} and median grainsize cannot be used to distinguish loess and palaeosols. This situation is different from that of CLP and Siberia. Though annual precipitation is low, soil moisture levels in Siberia may be high because of low temperatures and low evaporation rates. Furthermore, the subsoil is frozen, which prevents deep percolation of soil water and promotes waterlogging of the overlying soil, so the transformation of magnetic minerals occurs in the soils, while original magnetic components, with higher χ_{lf} are retained in the underlying loess.

However, in Dashing Rocks profile, there are fragipans and vertical gley veins (gammate structure) throughout the whole section (Tonkin *et al.* 1974; Xia *et al.* 1993), suggesting that it experienced a combination of vertical leaching and gleying, the effects of which were not only limited to the palaeosol layers, but also affected most loess layers. Furthermore, from Table 1, we know that the content of soft-magnetic minerals is very low in New Zealand source materials, and the original soft-magnetic components in loess were also further reduced by vertical leaching and gleying, just as in the palaeosols. This process makes χ_{lf} lower and χ_{lf} values of most layers similar. Thus, χ_{lf} loses its effectiveness as an indicator to distinguish loess and palaeosol layers. The uppermost soil layer is still in the accumulation period and the time over which it experienced magnetic minerals transformation is relatively short. Furthermore, it has good permeability, promoted by organic matter content, so it still retains some soft-magnetic minerals (such as magnetite) that cause the peak of χ_{lf}. The second loess layer is thick and porous, it also has a good permeability, moreover, there is blocky clay loam in the top of Loess Member 2, and this can prevent deep percolation of rainfall, so the original soft-magnetic component has been partly preserved and results in a peak of χ_{lf}. However, although the third
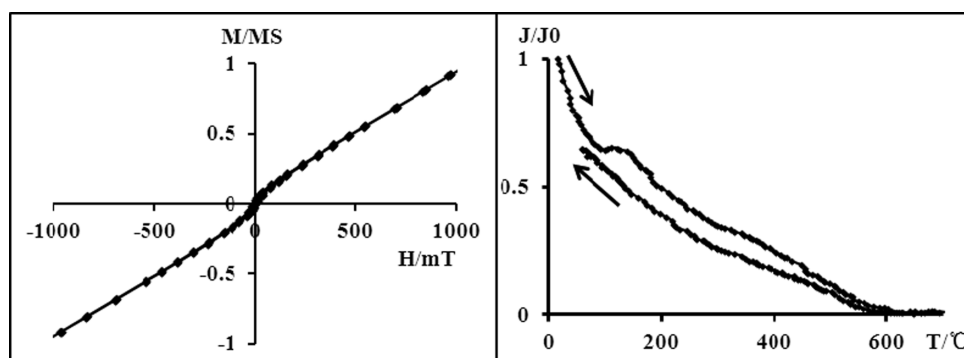
Figure 9. M_s–T curve and magnetic hysteresis loop of MWC sample from the lower part.

loess layer is the thickest, due to its prismatic fragipan structure, it has undergone strong vertical leaching, causing soft-magnetic minerals to be dissolved completely and there is no χ_{lf} peak. This can be confirmed from Figs 4–6: sample 22, from the second loess layer, has a soft-magnetic mineral content (indicated by hysteresis loops) which is higher than in samples 34 and 37 from the third loess layer. In addition, there is still a magnetite signal in sample 22 (Fig. 6), but no imprint exists in samples 34 and 37. Therefore, the strength of transformation after deposition has affected the χ_{lf} values.

6 CONCLUSIONS

(1) Based on an overall consideration of various magnetic parameters, the types of magnetic minerals in Dashing Rocks section are similar to those in CLP, but different in their proportions: The primary minerals are dominated by hard (goethite) and paramagnetic minerals, whereas soft-magnetic minerals (magnetite, maghemite) are very low.

(2) There are two reasons that cause χ_{lf} to be very low: (1) the χ_{lf} value of source material is low, and (2) magnetic mineral transformation during and after deposition is promoted by excessive moisture.

(3) In summary, high-effective soil moisture in Dashing Rocks profile has caused different layers to experience varying degrees of magnetic mineral transformation, and this is the main reason for the lack of correlation between χ_{lf} and pedogenic strength. Thus, for most loess layers, despite the climate during deposition being relatively arid, strong vertical leaching and gleying after deposition caused the original strong magnetic minerals to be largely dissolved or transformed, so χ_{lf} values of most loess and palaeosol layers are similar. The appearance of two χ_{lf} peaks can be attributed to the relatively weak strength of magnetic mineral transformation at those levels. Therefore, χ_{lf} has a complicated relationship with pedogenic environment, and we should be very careful when using it to infer past environmental changes.

ACKNOWLEDGEMENTS

REFERENCES

An, Z.S., 2000. The history and variability of the East Asian paleomonsoon climate, *Q. Sci. Rev.,* **19,** 171–187.

Banerjee, S.K., Hunt, C.P. & Liu, X.M., 1993. Separation of local signals from the regional paleomonsoon record of the Chinese loess plateau: a rock-magnetic approach, *Geophys. Res. Lett.,* **20,** 843–846.

Begét, J.E. & Hawkins, D.B., 1989. Influence of orbital parameters on Pleistocene loess deposition in Central Alaska, *Nature,* **337,** 151–153.

Begét, J.E., Stone, D.B. & Hawkins, D.B., 1990. Paleoclimatic forcing of magnetic susceptibility variations in Alaska loess during the late Quaternary, *Geology,* **18,** 40–43.

Berger, G.W., Pillans, B.J. & Tonkin, P.J., 2001. Luminescence chronology of loess-paleosol sequences from Canterbury, South Island, New Zealand, *New Zeal J. Geol. Geophys.,* **44,** 501–516.

Bidegain, J.C., Evans, M.E. & van Velzen, A.J., 2005. A magnetoclimatological investigation of Pampean loess, Argentina, *Geophys. J. Int.,* **160,** 55–62.

Bidegain, J.C. & Rico, Y., 2012. Magnetostratigraphy and magnetic parameters of a sedimentary sequence In Punta San Andres, Buenos Aires, Argentina, *Q. Int,* **253,** 91–103.

Bidegain, J.C., Rico, Y., Bartel, A., Chaparro, M.A.E. & Jurado, S., 2009. Magnetic parameters reflecting pedogenesis in Pleistocene loess deposits of Argentina, *Q. Int,* **209,** 175–186.

Bruce, J.G., Ives, D.W. & Leamy, M.L., 1973. Maps and sections showing the distribution and stratigraphy of South Island loess deposits, New Zealand Soil Survey Report 7.

Carter-Stiglitz, B., Banerjee, S.K., Gourlan, A. & Oches, E., 2006. A multi-proxy study of Argentina loess: marine oxygen isotope stage 4 and 5 environmental record from pedogenic hematite, *Palaeogeog. Palaeclimat. Palaeoecol.,* **239**(1–2), 45–62.

Chen, T., Xu, H., Xie, Q., Chen, J., Ji, J. & Lu, H., 2005. Characteristics and genesis of maghemite in Chinese loess and paleosols: mechanism for magnetic susceptibility enhancement in paleosols, *Earth planet. Sci. Lett.,* **240**(3–4), 790–802.

Chlachula, J., Evans, M.E. & Rutter, N.W., 1998. A magnetic investigation of a Late Quaternary loess/palaeosol record in Siberia, *Geophys. J. Int.,* **132**(1), 128–132.

Dalrymple, G.B., 1979. Critical tables for conversion of K-Ar ages from old to new constants, *Geology,* **7,** 558–560.

Dearing, J.A., Dann, R.J.L., Hay, K., Lees, J.A., Loveland, P.J., Maher, B.A. & O'Grady, K., 1996. Frequency-dependent susceptibility measurements of environment materials, *Geophys. J. Int.,* **124,** 228–240.

Deng, C., Vidic, N.J., Verosub, K.L., Singer, M.J., Liu, Q., Shaw, J. & Zhu, R., 2005. Mineral magnetic variation of the Jiaodao Chinese loess/paleosol sequence and its bearing on long-term climatic variability, *J. geophys. Res.-Solid Earth,* **110,** B03103, doi:10.1029/2004JB003451.

Evans, M.E. & Heller, F., 2001. Magnetism of loess/palaeosol sequences: recent developments, *Earth Sci. Rev.,* **54**(1–3), 129–144.

Florindo, F., Roberts, A.P. & Palmer, M.R., 2003. Magnetite dissolution in siliceous sediments, *Geochem. Geophys. Geosyst.,* **4,** 1053, doi:10.1029/2003GC000516.

Geiss, C.E., Egli, R. & Zanner, C.W., 2008. Direct estimates of pedogenic magnetite as a tool to reconstruct past climates from buried soils, *J. Geophys. Res.-Solid Earth,* **113,** B11102, doi:10.1029/2008JB005669.

Geiss, C.E. & Zanner, C.W., 2007. Sediment magnetic signature of climate in modern loessic soils from the Great Plains, *Q. Int.,* **162,** 97–110.

Hao, Q. & Guo, Z., 2005. Spatial variations of magnetic susceptibility of Chinese loess for the last 600 kyr: implications for monsoon evolution, *J. Geophys. Res.-Solid Earth,* **110,** B12101, doi:10.1029/2005JB003765.

Heil, C.W. Jr. *et al.*, 2010. Climatic interpretation of a 1.9 Ma environmental magnetic record of loess deposition and soil formation in the central eastern Pampas of Buenos Aires, Argentina, *Q. Sci. Rev.,* **29**(19–20), 2705–2718.

Heller, F. & Evans, M.E., 1995. Loess magnetism, *Rev. Geophys.,* **33**(2), 211–240.

Hu, S.Y., 1998. A magnetic study on lake sediments from Zoige Basin, Eastern Tibetan Plateau, China, *PhD thesis,* Universitaet Tuebingon, Attempto Service GmbH, pp. 79–83.

Imbrie, J. *et al.*, 1984. The orbital theory of Plesitocene climate: support from a revised chronology of the marine d^{18}O record, in *Milankovitch and Climate,* pp. 269–305, eds Berger, A., Imbrie, J., Hays, J., Kukla, G. & Saltzman, B. *et al.*, Reidel, Dordrecht.

Kemp, R.A., 2001. Pedogenic modification of loess: significance for palaeoclimatic reconstructions, *Earth Sci. Rev.,* **54**(1–3), 145–156.

Kravchinsky, V.A., Zykina, V.S. & Zykin, V.S., 2008. Magnetic indicator of global paleoclimate cycles in Siberian loess-paleosol sequences, *Earth planet. Sci. Lett.,* **265**(3–4), 498–514.

Kukla, G., Heller, F., Liu, X., Xu, T., Liu, T. & An, Z., 1988. Pleistocene climates in China dated by magnetic susceptibility, *Geology,* **16,** 811–814.

Lagroix, F. & Banerjee, S.K., 2002. Paleowind directions from the magnetic fabric of loess profiles in central Alaska, *Earth planet. Sci. Lett.,* **195**(1–2), 99–112.

Lagroix, F. & Banerjee, S.K., 2004. The regional and temporal significance of primary aeolian magnetic fabrics preserved in Alaskan Loess, *Earth planet. Sci. Lett.,* **225**(3–4), 369–385.

Liu, Q.S., Deng, C., Yu, Y., Torrent, J., Jackson, M.J., Banerjee, S.K. & Zhu, R., 2005. Temperature dependence of magnetic susceptibility in an argon environment: implications for pedogenesis of Chinese loess/palaeosols, *Geophys. J. Int.,* **161**(1), 102–112.

Liu, T.S. *et al.*, 1985. *Loess and the Environment,* Science Press, Beijing, pp. 1–481 (in Chinese).

Liu, X., Shaw, J., Liu, T., Heller, F. & Yuan, B., 1992. Magnetic mineralogy of Chinese loess and its significance, *Geophys. J. Int,* **108**(1), 301–308.

Liu, X., Liu, T., Hesse, P., Xia, D., Jiri, C. & Wang, G., 2008. Two pedogenic models for paleoclimatic records of magnetic susceptibility from Chinese and Siberian loess, *Sci. China (Ser. D),* **51**(2), 284–293.

Liu, X.M., Hesse, P. & Rolph, T., 1999. Origin of maghaemite in Chinese loess deposits: aeolian or pedogenic? *Phys. Earth planet. Inter.,* **112,** 191–201.

Liu, X.M., Hesse, P., Begét, J. & Rolph, T., 2001. Pedogenic destruction of ferrimagnetics in Alaskan loess deposits, *Aust. J. Soil Res.,* **39**(1), 99–115.

Liu, X.M., Liu, T., Xia, D., Hesse, P. & Chlachula, J., 2007. The analysis of two different pedogenesis models in reductive and oxidative conditions record by Chinese and Siberia Loess, *Sci. China (Ser. D),* **37**(10), 1382–1391.

Lü, H. & Han, J., 1994. Analysis on magnetism and paleoclimate meaning in modern soil of China. *Sci. China (Ser. B),* **24**(12), 1291–1297 (in Chinese).

Ma, M., Liu, X., Hesse, P., Lü, B., Guo, X. & Chen, J., 2013. Magnetic properties of loess deposits in Australia and their environmental signicance, *Q. Int.,* **926,** 198–205.

Maher, B.A., Mutch, T.J. & Cunningham, D., 2009. Magnetic and geochemical characteristics of Gobi Desert surface sediments: implications for provenance of the Chinese Loess Plateau, *Geology,* **37**(3), 279–282.

Maher, B.A. & Thompson, R., 1999. Palaeomonsoons I: the magnetic record of paleoclimate in the terrestrial loess and paleosol sequences, in *Quaternary Climates, Environments and Magnetism,* pp. 81–125, eds Maher, B.A. & Thompson, R., Cambridge University Press, Cambridge.

Maher, B.A., Thompson, R. & Zhou, L.P., 1994. Spatial and temporal reconstructions of changes in the Asian palaeomonsoon—a new mineral magnetic approach, *Earth planet. Sci. Lett.,* **125,** 461–471.

Maher, B.A., 1998. Magnetic properties of modern soils and Quaternary loessic paleosols: palaeoclimatic implications, *Palaeogeog. Palaeclimat. Palaeoecol.,* **137,** 25–54.

Matasova, G., Petrovský, E., Jordanova, N., Zykina, V. & Kapička, A., 2001. Magnetic study of Late Pleistocene loess/palaeosol sections from Siberia: palaeoenvironmental implications, *Geophys. J. Int.,* **147**(2), 367–380.

Mathews, W.H. & Curtis, G.H., 1966. Date of the Pliocene-Pleistocene boundary in New Zealand, *Nature,* **212,** 979–980.

McCraw, J.D., 1975. Quaternary airfall deposits of New Zealand. Quaternary Studied. Wellington, *Roy. Soc. New. Zeal.,* **13,** 35–44.

Minyuk, P.S., Subbotnikova, T.V. & Plyashkevich, A.A., 2011. Measurements of thermal magnetic susceptibility of hematite and Goethite, *Izv-Phys. Solid Earth,* **47**(9), 762–744.

Orgeira, M.J., Egli, R. & Compagnucci, R.H., 2011. A Quantitative model of magnetic Enhancement in loessic soils, in *The Earth's Magnetic Interior (IAGA Special Sopron Book Series),* Vol. **25,** pp. 361–398, Springer, Berlin.

Pillans, B. & Wright, I., 1990. 500,00-year paleomagnetic record from New Zealand loess, *Q. Res.,* **33,** 178–187.

Roberts, A.P., Cui, Y.L. & Verosub, K.L., 1995. Wasp-waisted hysteresis loops: mineral magnetic characteristics and discrimination of components in mixed magnetic systems, *J. Geophys. Res.,* **100**(B9), 17 909–17 924.

Runge, E.C.A., Walker, T.W. & Howarth, D.T., 1974. A study of late Pleistocene loess deposits, south Canterbury, New Zealand. Part 1. Forms and amounts of phosphorus compared with other techniques for identifing paleosols, *Q. Res.,* **4,** 76–84.

Sun, Y., Tada, R., Chen, J., Liu, Q., Toyoda, S., Tani, A., Ji, J. & Isozaki, Y., 2008. Tracing the provenance of fine-grained dust deposited on the central Chinese Loess Plateau, *Geophys. Res. Lett.,* **35,** L01804, doi:10.1029/2007GL031672.

Sun, J.M. & Liu, T.S., 2000. Multiple origins and interpretations of the magnetic susceptibility signal in Chinese wind-blown sediments, *Earth planet. Sci. Lett.,* **180,** 287–296.

Tauxe, L., Mullender, T.A.T. & Pick, T., 1996. Potbellies, wasp-waists, and superparamagnetism in magnetic hysteresis, *J. Geophys. Res.,* **101**(B1), 571–583.

Tonkin, P.J., Runge, E.C.A. & Ives, D.W., 1974. A study of late Pleistocene loess deposits, south Canterbury, New Zealand. Part 2. Paleosols and their strtigraphic implication, *Q. Res.,* **4,** 217–231.

Vander, M.H.U., 1951. Gamma ferric oxide in sediments, *J. Sediment. Res.,* **21,** 12–21.

Vandergoes, M.J. *et al.*, 2013. A revised age for the Kawakawa/Oruanui tephra, a key marker for the Last Glacial Maximum in New Zealand, *Q. Sci. Rev.,* in press. Available at http://dx.doi.org/10.1016/j.quascirev.2012.11.006.

Xia, D.S., Jia, J., Wei, H., Liu, X., Ma, J., Wang, X. & Chen, F., 2012. Magnetic properties of surface soils in the Chinese Loess Plateau and the adjacent Gobi areas, and their implication for climatic studies, *J. Arid Environ.,* **78,** 73–39.

Xia, Z., Bruce, J.G. & Crozier, M.J., 1993. Comparative study of New Zealand loess with China loess, *Acta Geographica Sinica,* **48**(4), 337–347 (in Chinese).

Zhou, L.P., Oldfield, F., Wintle, A.G., Robinson, S.G. & Wang, J., 1990. Partly pedogenic origin of magnetic variations in Chinese loess, *Nature,* **346,** 737–739.

Zhu, R.X., Shi, C., Suchy, V., Zeman, A., Guo, B. & Pan, Y., 2001. Magnetic properties and paleoclimatic implications of loess-paleosol sequence of Czech Republic, *Sci. China (Ser. D),* **44**(5), 387–394.

Zhu, R.X., Matasova, G., Kazansky, A., Zykina, V. & Sun, J., 2003. Rock magnetic record of the last glacial- interglacial cycle from the Kurtak loess section, Southern Siberia, *Geophys. J. Int.,* **152**(2), 335–343.